NASA TECHNICAL NOTE

NASA TN D-7433

NASA TN D-7433

CONTAMINATION ASSESSMENT AND CONTROL IN SCIENTIFIC SATELLITES

by Robert J. Naumann

George C. Marshall Space Flight Center
Marshall Space Flight Center, Ala. 35812

NATIONAL AERONAUTICS AND SPACE ADMINISTRATION • WASHINGTON, D. C. • OCTOBER 1973

TECHNICAL REPORT STANDARD TITLE PAGE

1. REPORT NO.	2. GOVERNMENT ACCESSION NO.	3. RECIPIENT'S CATALOG NO.
TN D-7433		

4. TITLE AND SUBTITLE	5. REPORT DATE
Contamination Assessment and Control in Scientific Satellites	October 1973
	6. PERFORMING ORGANIZATION CODE
7. AUTHOR(S)	8. PERFORMING ORGANIZATION REPORT #
Robert J. Naumann	M459
9. PERFORMING ORGANIZATION NAME AND ADDRESS	10. WORK UNIT NO.
George C. Marshall Space Flight Center Marshall Space Flight Center, Alabama 35812	11. CONTRACT OR GRANT NO.
	13. TYPE OF REPORT & PERIOD COVERED
12. SPONSORING AGENCY NAME AND ADDRESS	Technical Note
National Aeronautics and Space Administration Washington, D.C. 20546	14. SPONSORING AGENCY CODE

15. SUPPLEMENTARY NOTES

Prepared by Space Sciences Laboratory,
Science and Engineering

16. ABSTRACT

Techniques for assessment and control of the contamination environment for both particulates and condensible vapors in the vicinity of spacecraft are developed. An analysis of the deposition rate on critical surfaces is made considering sources within the line of sight of the surface in question as well as those obscured from the line of sight. The amount of contamination returned by collision with the surrounding atmosphere is estimated. Scattering and absorption from the induced atmosphere of gases and particulates around the spacecraft are estimated. Finally, design techniques developed for Skylab to reduce the contamination environment to an acceptable level are discussed.

17. KEY WORDS	18. DISTRIBUTION STATEMENT
	Distribution Category: 30

19. SECURITY CLASSIF. (of this report)	20. SECURITY CLASSIF. (of this page)	21. NO. OF PAGES	22. PRICE
Unclassified	Unclassified	41	Domestic, $3.00 Foreign, $5.50

For sale by National Technical Information Service, Springfield, Virginia 22151

TABLE OF CONTENTS

LIST OF ILLUSTRATIONS

LIST OF TABLES

CONTAMINATION ASSESSMENT AND CONTROL IN SCIENTIFIC SATELLITES

I. INTRODUCTION

As space experiments develop in complexity and sophistication, the problems of interference from the self-induced local environment become more severe. Extreme care in design and operational procedure is demanded to insure that the experiments measure the intended phenomena rather than extraneous self-induced environmental effects. Optical experiments, particularly those operating in the far ultraviolet, are highly susceptible to contamination from self-induced atmosphere; hence, the study of such interference is referred to as "Optical Contamination" or, in a more general sense, "Contamination."

Several experiments on both manned and unmanned spacecraft have failed or have been severely degraded because the effects of contamination were not considered. Scattered light from ice crystals or other debris has prevented astronomical observations in the sunlit portion of the orbit. Windows and other optical surfaces have become coated with contaminating films and globules which cause scattering and absorption. Since organic molecules are particularly good absorbers in the far ultraviolet, a film of only a few monolayers can destroy the usefulness of a mirror or grating. Cooled infrared detectors have become coated with layers of ice from condensing water vapor. Mass spectrometers have become swamped by water vapor and other outgassing products. High voltage power supplies have been destroyed by arc-over because the ambient pressure was not yet below the corona region when the high voltage was activated. Such difficulties are not restricted to the operation of experiments in space; many optical surfaces have become contaminated in vacuum chambers during tests.

This type of problem was recognized as being extremely critical to the Apollo Telescope Mount (ATM) experiments and other Skylab experiments. Since ATM must operate in the sunlight portion of the orbit, the problem of scattering from particulate debris cannot be avoided. Therefore, it is mandatory that extreme care be taken to prevent the production of particulates. Also, since many of the measurements are made in the extreme ultraviolet where obtaining good reflectivity is a difficult problem, the deposition of even a few monolayers of an organic contaminant cannot be tolerated. For this reason, extreme care must be exercised in the selection of nonmetallic material to be used in the vicinity of optics. Also, elaborate precautions must be taken in storage and during vacuum testing of the optics to prevent deposits of dust particles, outgassing products, and vacuum pump oil. All structures must be as dust free as possible to prevent such particles from forming a debris cloud in orbit or deposition on the optics during boost. Care must be taken to vent all possible sources of outgassing material and regions that contain trapped atmospheric gases so that pressures in the vicinity of high voltage systems will rapidly fall well below the corona regime, and measurements for verifying that the pressure is in fact low enough are required before activation of high voltage systems.

A physical basis for estimating and controlling the contamination problems that may be encountered in scientific satellites, both manned and unmanned, are developed in this report. Primary emphasis is placed on Skylab and the contamination countermeasures developed for it.

II. DEPOSITION OF CONTAMINANTS

The possibility of vapor deposition of high molecular weight polymeric fragments on critical surfaces must be considered. Typical damage produced by thin contaminant films on grazing incidence X-ray optics [1] is shown in Figure 1. Since organic molecules absorb strongly in the ultraviolet, thin films can also cause severe degradation in ultraviolet optics. Furthermore, since deposited films, because of the surface mobility of the molecules, tend to cluster about active sites such as dislocations or other surface imperfections, even visible optical surfaces can be degraded by unwanted scattering. Water vapor, which is usually the most abundant species of vapor, does not cause problems with warm optics but can cause severe degradation of cooled infrared detectors.

A. Fundamental Principles

It is well to review a few fundamentals of surface physics and kinetic theory which govern the deposition of contaminants.

The deposition rate $\dot{\sigma}$ is related to the incident flux n by

$$\dot{\sigma} = n - \frac{\sigma}{\tau} \tag{1}$$

where σ is the surface density and τ is the stay time of the molecule on the surface.

The stay time is given by the Frenkel relation

$$\tau = \tau_o e^{H_v/RT} \tag{2}$$

where τ_o is the vibrational period of the lattice, usually taken to be 10^{-13} sec; H_v is the heat of adsorption or surface binding energy; and T is the absolute temperature.

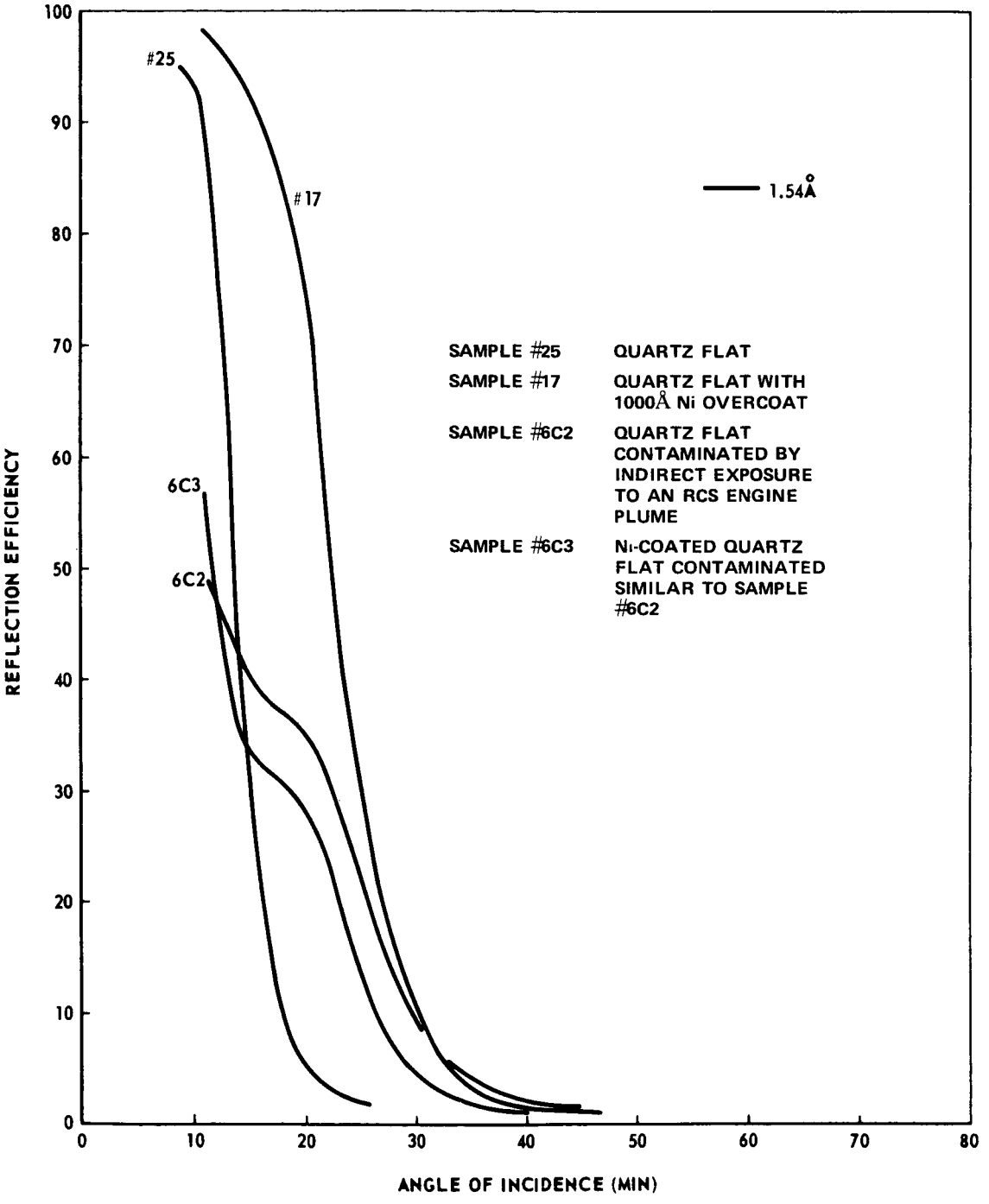

Figure 1. Reflection efficiency for grazing incidence 1.54-Å X rays.

The primary interest is in situations that lead to continuous buildup of contamination layers (see Appendix A). After the first few monolayers have been deposited, the surface in question is assumed to have the same properties except for temperature as the source of contaminant. The σ in equation (1) becomes a constant σ_s given by

$$\sigma_s = \left(\frac{N_A \rho}{M}\right)^{2/3} \tag{3}$$

where N_A is the Avogadro number, ρ is the bulk density, and M is the molecular weight.

A parameter of interest in selecting materials for space applications is the measured mass loss at some given temperature, T_{ref}. This mass loss is $-\dot{\sigma}$ in equation (1) times the mass of the molecules (M/N_A) with the incident flux $n = 0$. The stay time at T_{ref} can be found from

$$\tau_{ref} = \frac{\sigma_s M}{N_A \dot{m}} \quad . \tag{4}$$

The stay times at any other temperature can be found by eliminating H_v from the Frenkel relation, giving

$$\tau = \tau_o \left(\frac{\tau_{ref}}{\tau_o}\right)^{T_{ref}/T} \quad . \tag{5}$$

B. Internal Sources

Consider a container of volume V with a number of surfaces with areas A_i and temperatures T_i. The change in number density N is given by

$$\dot{N} = -\sum_i \frac{\dot{\sigma}_i A_i}{V} \tag{6}$$

where $\sigma_i A_i$ is the net increase of molecules on surface A_i. Using equation (1) and the kinetic theory relationship between flux and density,

$$n = \frac{Nv}{4} \quad , \tag{7}$$

the steady state value for N is obtained by setting $\dot{N} = 0$, giving

$$N = \frac{4\sigma_s}{v} \frac{\sum_i (A_i/\tau_i)}{\sum_i A_i} \quad . \tag{8}$$

The average molecular speed is given by

$$v = \sqrt{\frac{8RT}{\pi M}} \quad . \tag{9}$$

The rate of growth on the jth surface can be found by inserting the results of equations (7) and (8) into equation (1):

$$\dot{\sigma}_j = \sigma_s \left(\frac{\sum_i (A_i/\tau_i)}{\sum_i A_i} - \frac{1}{\tau_j} \right) \quad , \tag{10}$$

or the time for a monolayer to grow on surface 1 is given by

$$t_1 = \frac{\sigma_s}{\dot{\sigma}_s} = \frac{\tau_1 A_T}{A_2\left(\frac{\tau_1}{\tau_2} - 1\right) + A_3\left(\frac{\tau_1}{\tau_3} - 1\right) + \ldots} \quad . \tag{11}$$

If t_1 is negative, the contamination film is evaporating faster than it is being deposited. The number of monolayers at equilibrium is given by equation (A-1); equation (A-2) represents the maximum number of monolayers possible.

As an illustrative example, consider a cylindrical container 30 cm in diameter by 100 cm long. Let one end be an open aperture and the other end contain an optical surface, say a telescope mirror. The source of contaminant in this case is assumed to be an insulated wire in the canister, 1 mm in diameter and 2 m long. The wire is assumed to be operating above ambient temperature because of the current it is carrying. Good insulations have an outgassing rate of $\sim 3 \times 10^{-11}$ gm/cm^2/sec at 50°C. A wire with "bad" insulation that has 10 times this outgassing rate is also considered for comparison. The times required for deposition of a monolayer are given in Table 1 for a variety of mirror and wall temperatures. Also shown is the case where it is assumed that the binding energy of the deposit on the mirror surface is increased approximately 5-fold to 5 eV/atom or 115 Kcal/mole. Such values are typical for chemical bonds that could be formed by photolytic ploymerization or

TABLE 1. TIMES REQUIRED FOR DEPOSITION OF A MONOLAYER

	T_S = 323° K "Good" Insulation	T_S = 333° K "Good" Insulation	T_S = 323° K "Bad" Insulation	T = 333° K "Bad" Insulation
Walls at 300° K, mirror at 300° K, aperture closed	3.9 days (0.256 t)	1.2 days (0.833 t)	8.8 hr (2.73 t)	13.34 min (10.8 t)
Walls at 300° K, mirror at 300° K, aperture open	12.04 days (0.083 t)	1.54 days (0.650 t)	2.1 days (0.476 t)	4.3 hr (5.58 t)
Walls at 300° K, mirror at 299° K, aperture open	2.51 days (0.398 t)	23.3 hr (1.03 t)	6.0 hr (4.00 t)	2.6 hr (9.23 t)
Walls at 299° K, mirror at 300° K, aperture open	-4.8 days (12.8)	1.04 days (0.961 t)	-8.5 hr (11.3)	10.52 hr (2.28 t)
Walls at 300K, mirror at 300K, 5 eV/atom binding, aperture open	9.3 hr (2.58 t)	7.6 hr (3.16 t)	47.5 min (30.3 t)	40.7 min (35.4 t)

$A_{wall} = 9424\ cm^2$

$A_{mirror} = 707\ cm^2$

$A_{aperture} = 707\ cm^2$

$A_{source} = 62.8\ cm^2$

"Good" insulation has $\dot{m} = 3 \times 10^{-11}$ gm/cm² /sec, M = 100, ρ = 1 gm/cm³

"Bad" insulation has $\dot{m} = 3 \times 10^{-10}$ gm/cm² /sec, M = 100, ρ = 1 gm/cm³

Note: The numbers in parenthesis represent the number of monolayers grown in t days. For negative values of t_1, the value in the parenthesis represents the maximum number of monolayers predicted from the BET equation with C large.

other chemisorption on the surface. The stay time for this binding energy at ambient temperature is 10^{71} sec, which is for all purposes infinite. For this, equation (11) becomes

$$t_1 = \frac{A_T}{A_2/\tau_2 + A_3/\tau_3 + \ldots} \quad . \tag{12}$$

Several observations are in order. The effect of increasing the mirror temperature above the surrounding walls results in an evaporation of the contaminant film in all but the worst cases. Use of a "bad" insulation greatly increases the rate of contaminant deposit in all cases, but the optic will clean itself far more rapidly. If chemisorption takes place on the surface of interest, very rapid buildup will result and the optic will never clean itself.

This treatment assumed a randomized velocity and is invariant with geometry. For sources situated such that the surface of interest subtends a large solid angle, the geometrical treatment described in the following section should be used.

C. External Sources

For an external source such as a solar cell panel, the flux at some point in its line of sight is given by

$$n = \frac{n_{evap}}{\pi} \int_{\Omega} \cos\theta_1 \, d\omega \tag{13}$$

where θ_1 is the angle between the surface in question and the line of sight to the source, and Ω is the solid angle subtended by the source. If the solid angle is small, θ_1 is constant and this reduces to

$$n = \frac{n_{evap} A_\perp}{\pi r^2} \quad . \tag{14}$$

After the first monolayer is formed, the deposition rate is given by equation (1):

$$\dot{\sigma}_1 = n_{evap} \frac{A_\perp}{\pi r^2} - \frac{\sigma_s}{\tau_1} \quad . \tag{15}$$

Since $n_{evap} = \sigma_s/\tau_2$

$$\dot{\sigma} = \sigma_s \left(\frac{A_\perp}{\pi r^2 \tau_2} - \frac{1}{\tau_1} \right) \tag{16}$$

where τ_1 and τ_2 are given by equation (5).

Since $A_\perp/\pi r^2$ is usually small, τ_2 must be $\ll \tau_1$ if the contaminated surface is to gain mass. In fact, from equation (13) no mass will deposit unless $\tau_2 < \tau_1$. This generally means the source must be considerably hotter than the collecting surface.

McKeown [2] using a quartz crystal microbalance on OGO-6 measures a flux of 9.2×10^{-11} gm/cm^2/sec from solar cells that subtended an area of 2.23 m^2 at a distance of 3.05 m. Later, when the sensors looked toward space, he observed an evaporation rate of 1.2×10^{-13} gm/cm^2/sec for a temperature of 7°C. From this, he estimated a heat of absorption of 26 Kcal/mole, which is typical of polymers found in solar cell assemblies. The calculated flux for different solar cell temperatures is shown in Figure 2. It may be seen that a solar cell temperature of 70°C is required to produce the observed flux.

The deposition rates produced by this flux on a surface at various temperatures are given in Table 2 along with the time required to form a monolayer. It may be seen that the surface must be cooler than 60°C in order to collect contaminants.

D. Return Mechanisms

There has been much concern over the induced atmosphere surrounding a spacecraft. The gaseous component for the most part is directed radially and expanding freely. There are only two mechanisms that have any reasonable chance of redirecting the molecules back to the spacecraft in any significant flux: scattering from the ambient atmosphere and self-scattering between out-going molecules.

1. Atmospheric Scatter. The probability of return of a molecule by atmospheric scattering at the stagnation point is [3] (see Appendix B)

$$\frac{n_{ret}}{n_{out}} = \frac{R_o N_a v_a \sigma_a}{v_r} \left(\frac{\pi^2 - 4}{8} \right) \tag{17}$$

where v_r is the radial velocity, ~400 m/sec; v_a is the satellite velocity, ~8000 m/sec; σ_a is the scattering cross section, $\sim 1.04 \times 10^{-19}$ m^2; N is the ambient density at 420 km, $\sim 1.5 \times 10^{14}$ m^{-3}; and R_o is the spacecraft radius, ~10 m. For these values,

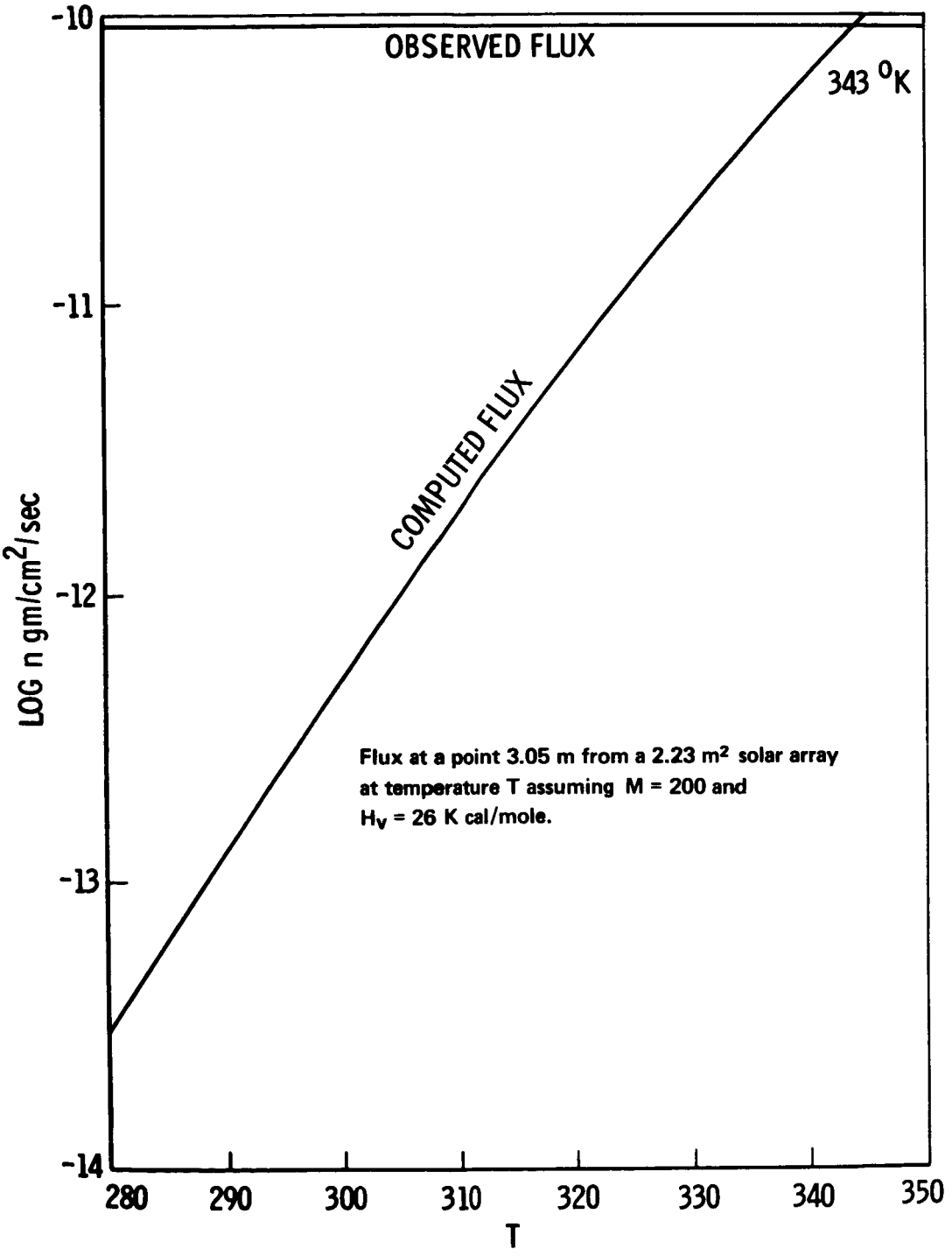

Figure 2. Computed outgassing flux from OGO-6 solar cells as a function of temperature. (The observed value was inferred from McKeown's quartz microbalance measurements when the solar cell temperature was 72°C. McKeown also reports an order of magnitude drop in flux as the solar cells drop to 60°C.)

TABLE 2. DEPOSITION RATE AND TIME PER MONOLAYER FOR INCIDENT FLUX OF 9.2×10^{-11} gm/cm^2/sec AS FUNCTION OF COLLECTOR SURFACE TEMPERATURE

T(° K)	$\dot{\sigma}$(gm/cm^2/sec)	t_1(sec)
280	9.19×10^{-11}	753
290	9.14×10^{-11}	757
300	8.98×10^{-11}	771
310	8.41×10^{-11}	823
320	6.54×10^{-11}	1058
330	8.47×10^{-12}	8174
340	-1.53×10^{-10}	-452 (1.6)
350	-5.86×10^{-10}	-118 (1.2)

Note: Numbers in parenthesis represent the maximum number of monolayers at equilibrium.

$$\frac{n_{ret}}{n_{out}} = 0.0023$$

Typical outgassing rates for Skylab are:

0.208 gm/sec H_2O

0.135 gm/sec $O_2/N_2/CO_2$

0.008 gm/sec outgassing products.

Table 3 gives itemization of the sources.

For the outgassing products, assume M = 200. This represents 2.4×10^{19} molecules/sec. Taking the spacecraft to be a sphere 20 m in diameter, the surface area is 1.25×10^7 cm^2. The average efflux is, therefore, 1.9×10^{12} mol/cm^2/sec. The return flux

TABLE 3. LIFE SUPPORT SYSTEM

Leakage	14.7	lb/day	N_2/O_2
Molecular sieve	7.7	lb/day	H_2O
	3.3	lb/day	N_2/O_2
	6.8	lb/day	CO_2
Trash lock	0.006	lb/day	H_2O
	0.64	lb/day	N_2/O_2
ECS	9.1	lb/day	H_2O
Wash H_2O	6	lb/day	H_2O
Waste	5	lb/day	H_2O
Urine	9.5	lb/day	H_2O + vapors
Fecal	2.3	lb/day	H_2O + vapors
Totals			
0.98 gm/sec (18.64 lb/day) N_2/O_2 [a]			
0.208 gm/sec (39.60 lb/day) H_2O			
0.035 gm/sec (6.8 lb/day) CO_2			
0.341 All gasses			

a. 30 percent N_2 ; 70 percent O_2

at apex is $n_{ret} = 4.4 \times 10^9$ mol/cm^2/sec. Since the surface density $\sigma_s = 2.08 \times 10^{14}$ mol/cm^2, the time to form a monolayer would be 13.25 hr, provided every incident molecule was permanently chemisorbed on the surface. If the molecules are to strike the surface faster than they leave, they will require stay times equal to this amount. The time to grow a monolayer for various temperatures is estimated in Table 4, assuming the same H_v as that observed by McKeown.

For H_2O, the return flux at the stagnation point is 1.28×10^{12} mol/cm^2/sec. Since σ_s is 1.038×10^{15} mol/cm^2, the required stay time to cause buildup is 810 sec. The stay time for H_2O is given empirically by

$$t = 1.05 \times 10^{-16} \; e^{6049/T} \quad . \tag{18}$$

Therefore, T would have to be lower than 139° K to allow H_2O buildup at this flux.

TABLE 4. TIME FOR MONOLAYER FORMATION FROM ATMOSPHERIC BACKSCATTER AT THE STAGNATION POINT

T(° K)	τ_1	t_1	(σ/σ_S) equil.
280	31.15 day	13.36 hr	1.8 t (days)
290	6.66 day	14.30 hr	1.7 t (days)
300	1.58 day	20.08 hr	1.2 t (day)
310	9.85 hr	-1.64 day	4.0
320	2.78 hr	-3.52 hr	1.3

Assumptions:

1. Material M = 200 evaporate at 1.2×10^{-13} gm/cm^2/sec at 290° K.
2. Mass is lost at 0.008 gm/sec.
3. Return fraction is 0.0023.

H_2O can cause problems with extremely cold surfaces, such as cooled detectors. The tolerable flux of H_2O vapor as a function of detector temperature is given by

$$n = \frac{\sigma_s}{\tau} = \frac{1.038 \times 10^{15} \text{ mol/cm}^2/\text{sec}}{1.05 \times 10^{-16} \; e^{6049/T}} \quad .$$

The tolerable fluxes for H_2O vapor are given in Table 5.

The returning molecules from atmospheric scatter will be fairly energetic, having collided with relative velocities of 8 km/sec. This is equivalent to temperatures in excess of 50 000° K or more than 5 eV. Chemical changes will certainly take place, and the returning molecules may be lighter fragments, free radicals, ions, or atomic species. It is possible that

TABLE 5. TOLERABLE FLUXES FOR H_2O VAPOR

T(° K)	n(mol/cm^2/sec)[a]	n*(mol/cm^2/sec)[b]
4	0	1.2×10^{10}
70	2.9×10^{-7}	1.2×10^{10}
100	5.3×10^{4}	1.2×10^{10}
150	3.0×10^{13}	3.0×10^{13}
200	7.2×10^{17}	7.2×10^{17}
273	2.3×10^{21}	2.3×10^{21}

a. n represents the tolerable flux for no buildup.
b. n* represents a buildup of 1 monolayer/day.

some of the species may chemically combine with the surfaces, but the impact energy is so high that they will probably be more effective in cleaning the surface rather than contaminating it. In addition, the atmospheric flux of 1.2×10^{14} mol/cm^2/sec at 420 km will also cause sputtering. McKeown [4] observed an additional mass loss rate of 2.3×10^{-13} gm/cm^2/sec when his detector was oriented toward the velocity vector. From this he calculates a sputtering yield of 7×10^{-5} molecules of contaminant per atmospheric collision.

2. Self-Scattering. Self-scattering, or scattering between molecules leaving the spacecraft, is difficult to calculate properly. A very crude model is described here which places an upper limit on the return flux by making some gross assumptions.

First, assume that the density at r is given by

$$N(r) = \frac{n_{total}}{v_r} \frac{R^2}{r^2} \tag{19}$$

where v_r is the average radial velocity and n_{total} is the total number of molecules per unit time divided by the total area of the spacecraft taken to be a sphere of radius R. The collisions per unit volume at r between these molecules and a flux of a specific species, $n(r) = n_{out} R^2/r^2$ is

$$d\dot{Q} = n(r)\, N(r)\, \sigma_a\, dV \quad .$$

The probability of return is dependent on the collision angle and the center of mass velocity, which is always positive radially. This fact greatly restricts the probability of return, but even a first order attempt to include this involves tedious computation. A gross estimate simply assumes the scatter is isotropic in the lab system and the return probability is $\omega/4\pi$ where ω is the solid angle subtended by the spacecraft. This, of course, greatly overestimates the return probability. Therefore, the return flux is

$$4\pi R^2 n_{ret} = \int_R^\infty \frac{\omega}{4\pi} n(r) N(r) \sigma_a 4\pi r^2 dr \tag{20}$$

$$\frac{n_{ret}}{n_{out}} = \int_R^\infty \frac{\pi R^2}{4\pi r^2} \frac{n_{total}}{v_r} \frac{R^4}{r^4} \sigma_a \frac{r^2}{R^2} dr \tag{21}$$

$$\frac{n_{ret}}{n_{out}} = \frac{R\, n_{total}\, \sigma_a}{12\, v_r} \tag{22}$$

Notice that the probability of return is a function of the total molecular outflow. Using

$R = 10$ m

$\sigma_a = 1.04 \times 10^{-19}$ m^2

$v_r = 400$ m/sec ,

$n_{total} = 5.12 \times 10^{18}$ mol/m^2/sec .

The n_{total} includes all the molecules leaving the spacecraft. The return probability is

$$\frac{n_{ret}}{n_{out}} = 0.0011$$

which is about half the atmospheric-scattered contribution at the stagnation point. Remember, however, that the component from atmospheric scattering falls off rapidly away from the stagnation point and becomes zero at the antivelocity vector, whereas the self-scattering component is uniform in direction. Also, the returning molecules have ambient temperatures and have not suffered energetic collisions.

3. Other Return Mechanisms. Some speculation has been advanced concerning the possibility of the spacecraft "dragging" its contamination cloud along with it through charge or dipole interactions. This does not seem feasible for the following reasons. First, the molecules would either have to be charged or have dipole moments. Hoffman [5], with his Apollo 15 and 16 mass spectrometers which looked away from the spacecraft, detected neutral CO_2 which is not a polar molecule. Second, charges on spacecraft are never more than a few volts because of the large discharge currents produced by the ionosphere or the solar plasma. Only the solar plasma can provide currents as high as 10^{-7} amps/m^2, which would discharge a 2-m diameter sphere at the rate of 20 000 volts/sec [6]. Therefore, even if the spacecraft takes on a high potential by firing a thruster or dumping a liquid, it will soon return to equilibrium. Finally, the Deybe length is only a few centimeters in the ionosphere and a few meters in cislunar space. Therefore, the particle would not be influenced by any spacecraft charge at any great distance. Since ion production rates are generally less than $10^2/cm^3/sec$ at 350 km where the density is 4×10^8 molecules/cm^3, the lifetime before ionization must be 4×10^6 sec. By this time, the molecule should be far enough away to be completely screened from the spacecraft potential.

E. Methods of Control

Having established in the previous discussion the general behavior of contamination deposition, methods of controlling may be considered. Perhaps the most obvious step is to eliminate or carefully control the use of nonmetallic materials. Most agencies have their own specification for acceptance or rejection of materials. These are generally based on steady state weight loss at elevated temperatures, amount of condensing material on a cold surface near the heated sample, n_o mass fragments above a certain molecular weight, etc. These tests represent screening methods to eliminate the worst offenders, which is necessary as seen from the previous examples. However, there is a tendency to lose sight of the fact that the criteria are somewhat arbitrary and that "acceptable" materials still cause contamination.

Careful consideration must be given to the intended use, the amount used, the location relative to critical surfaces, and, above all, the maximum expected temperature of the material. Wires and electronic components that dissipate heat demand special care. They will be the primary internal sources. They should never be allowed to be in direct line of sight with a sensitive surface. The very stable polymers used in insulation and paints with low outgassing properties will still come off at elevated temperatures in sufficient quantities to cause problems to nearby surfaces in their direct line of sight. Because of their stability, they will be extremely persistent if they do condense on a cold surface. Keeping the surface in question at a higher temperature than its surroundings is an excellent way to protect it from contamination. As given in Table 1, only a $\pm 1^\circ$ difference in temperature relative to its surroundings determines whether a surface contaminates rapidly or cleans itself.

It is even better practice to isolate optical surfaces from sources of contamination by shrouding them directly to the outside by means of an unpainted metal tube. The OAO is designed this way (Fig. 3) and operates with its mirrors at -45°C. There has been no degradation in the optical system in its several years of operation. Since ATM was not designed this way (Fig. 4), much more care was necessary in controlling the choice, placement, handling, and cleanliness of all material used in the canister. All nonmetallic components go through a thermal vacuum bake before they are installed to eliminate some of the initial outgassing. All handling and assembly of the internal portions of ATM is done in a class 10K clean room, while the external portions are assembled in a class 100K clean facility.

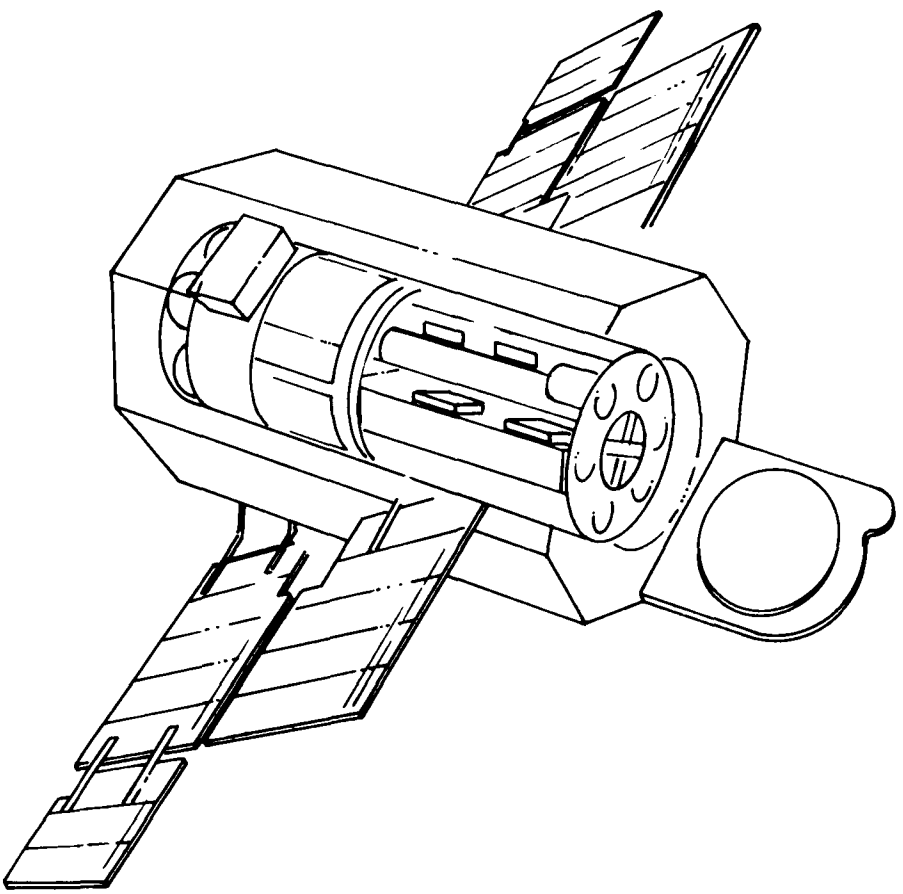

Figure 3. The OAO-2 spacecraft showing internal location of experiments. (All optical surfaces are located in tubes which isolate them from the interior of the spacecraft.)

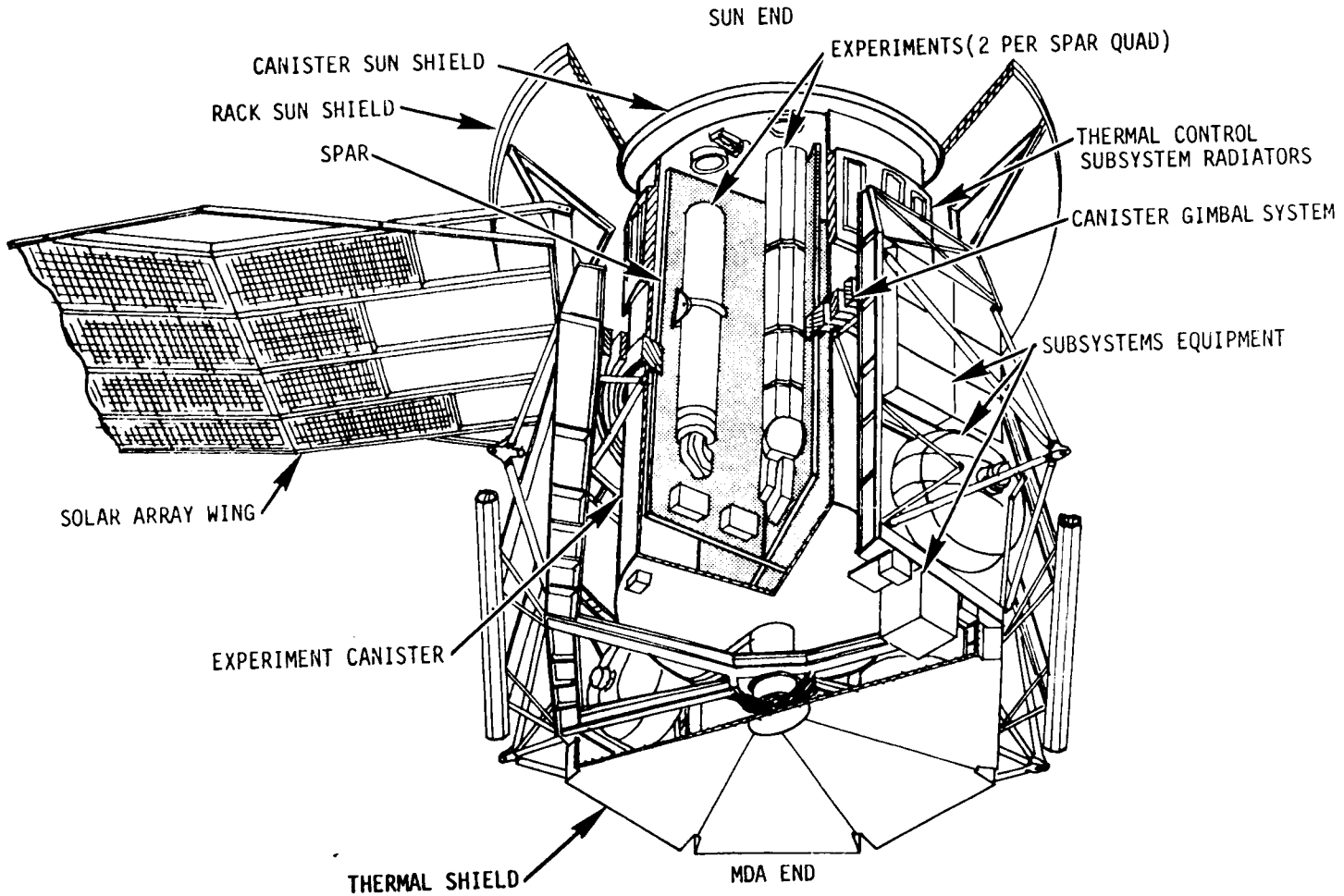

Figure 4. The interior of the ATM. (Although optical surfaces are shrouded from direct line of sight to external sources, they are not coupled directly to the sunshield. Therefore, they will be subjected to the gaseous environment of the interior of the canister.)

Particular care must be exercised in venting regions around high voltage components. Potting voids and poorly vented regions or sheets of multilayer insulation opening near high voltage components have damaged or destroyed a number of experiments from high voltage arcing. Because of the open window phototubes and large amounts of multilayer insulation in ATM, pressure gages have been installed to assure that the pressure is below the corona region before activating the high voltage system.

Cooled detectors required for infrared experiments are especially susceptible to contamination, particularly from H_2O vapor. Again, the multilayer insulation usually used to insulate the detector is the source of a large quantity of trapped H_2O vapor. Care must be taken to vent this away from the detector surface.

Finally, care must be taken to locate vents, RCS thrusters, or other sources of expelled material such that the plume does not contact the surface. Whether suitably located RCS thrusters can be operated without contaminating extremely sensitive optics is still questionable. A decision was made early in the Skylab program to avoid this problem by using cold gas thrusters to desaturate the CMG's. The J series Apollo vehicles use RCS engines without apparent damage to the SIM Bay experiments; however, the thrusters that fire over the SIM Bay are inhibited when the SIM Bay is open. There is a certain amount of splatter from liquid dump plumes. Astronauts on Apollo flights report seeing ice crystals from liquid dumps strike the CM windows; whether material from the RCS engines does this is not yet known. It is known that a thin liquid film of very low vapor pressure is ejected from the perimeter of the nozzle. It would appear best at this time to avoid firing of RCS thrusters when critical surfaces are exposed and to provide some means of covering these surfaces during RCS maneuvering.

III. INDUCED ATMOSPHERE

The second concern in conducting optical experiments from a spacecraft is the effect of the atmosphere surrounding the spacecraft on the intended observations. This atmosphere will consist of mostly molecular species such as O_2, CO_2, N_2, and H_2O which originate from outgassing, leakage, purges, waste dumps, and thruster firings. A smaller amount of higher molecular weight material is present from outgassing of nonmetallic material in the spacecraft. Also present will be particulate matter which may come from dust from the surface or interior of the spacecraft, flakes of paint and insulation material, and ice crystals from H_2O jettisoned into vacuum. The effects of concern are absorption and scattering of radiation which may interfere with optical experiments. Scattering from particulates is especially troublesome. On several occasions, star trackers have been known to lose their reference star and track a small bright particle instead. No dim light astronomical observations have been possible from spacecraft during sunlight because of unwanted scattering from particulates and/or structure.

A. Column Densities

The most significant parameter of the induced atmosphere is the column density N_c. For an isotropic source of material with radius R,

$$N_c = \frac{\dot{N}_s}{4\pi R v_r}$$

where $\dot{N}_s$ is the source rate (number/unit time), R is the radius, and v_r is the average radial velocity.

For a point source with a Lambertian distribution, such as a vent or leak, a more general expression is

$$N_c = \frac{\dot{N}_s \cos\gamma}{\pi v_r} \left\{ \frac{1}{R_r} - \frac{1}{R_f} - \frac{1}{R_o} \left(\sqrt{\frac{R_1^2}{R_o^2} - 1} \right) \left(\sqrt{1 - \frac{R_o^2}{R_f^2}} - \sqrt{1 - \frac{R_o^2}{R_r^2}} \right) \right\}$$

where

$R_f = v_r t_1$; R_1'; R_1 (whichever greater),

$R_r = v_r t_2$; R_1'; R_1 (whichever greater),

γ is the angle between the plume axis and the line of sight, R_o is a vector from the nozzle to the sight vector making a right angle with the sight vector, R_1 is a vector from the sight vector to the nozzle making a right angle with the nozzle axis, R_1' is the distance from the nozzle to viewing port if the viewing port is in front of the nozzle plane (otherwise $R_1 = R_1'$), t_1 is the time the vent was initiated, and t_2 is the time it was terminated ($t_2 = 0$ if not terminated). This expression allows the computation of the column density as a function of time for each vent location and can predict clearing times of steady state values.

For molecules, the velocities are of the order of 400 m/sec. However, predictions of velocities for particulates are difficult. Photographs of Apollo water dumps indicate an approximate velocity of 6 m/sec for the ice crystals [7]. Dust particles leaving the spacecraft probably have much less velocity. If it is necessary to include a distribution of velocities, this equation must be integrated over the velocity distribution.

For Skylab, the column densities resulting from the various vents seen from the ATM are summarized in Table 6. It may be seen that the molecular column densities from induced atmosphere are substantially less than the 6.3×10^{14} molecules/cm^2 from residual atmosphere at 420 km.

TABLE 6. SCATTERING FROM INDUCED ATMOSPHERE AT $\theta = 0$

Source	Source Rate (gm/sec)	N_c (No./cm^2)	$(d\sigma/d\Omega)_o$ (cm^2)	$B/B_\odot$
All condensate water in 1-μ sphere	0.05	1.26×10^{4}	2.47×10^{-8}	1.7×10^{-8}
All condensate water in 10-μ spheres	0.05	1.26×10^{1}	2.47×10^{-4}	1.7×10^{-7}
All condensate water in 100-μ spheres	0.05	1.26×10^{-2}	2.47×10^{-1}	1.7×10^{-6}
Actual particles from vent	10^{-11}	1.5×10^{-7}	2.47×10^{-8}	2.2×10^{-19}
All gasses (visible)	0.349	1.90×10^{13}	7.7×10^{-28}	1.9×10^{-19}
Cabin gasses, X ray (Z = 18)	0.341	1.85×10^{13}	2.57×10^{-23}	2.8×10^{-14}
Outgas products, X ray (Z = 2400)	0.008	1.31×10^{11}	4.58×10^{-19}	3.6×10^{-12}
1-μ dust layer leaving in 7 days	0.001	1.64×10^{4}	2.47×10^{-8}	2.4×10^{-8}
Dust from 1 yr in 100-K environment leaving in 7 days	5.72×10^{-5}	56	1.39×10^{-6}	4.7×10^{-9}

For Reference

Source	$B/B_\odot$
Near solar corona (K+F)	4.9×10^{-6}
Zodiacal light (10°)	1.3×10^{-11}
Gegenschein	9.1×10^{-14}
Perfect sky from ground (zenith)	1.5×10^{-14}
Unresolved stars (fainter than $M_V = 6$)	3.4×10^{-14}
Galactic and zodiacal background	2.0×10^{-14}

B. Absorption

Given the column density, the spectral absorption may be computed from

$$I(\lambda) = I_O(\lambda)\, e^{-\sigma_\lambda N_c}$$

where σ_λ is the absorption cross section for the wavelength of interest. Typical values of σ_λ are given [8] in Table 7 along with the $\Delta I/I_o$ for ATM. It may be seen that the absorption effect for the induced atmosphere is negligible.

TABLE 7. ABSORPTION FROM EXPELLED GASSES

Gas	Source Rate (gm/sec)	N_c (No./cm^2)	σ_{max} (Mb)	λ_{max} (Å)	$\Delta I/I_o$
N_2	0.029	1.3×10^{12}	144	970	0.00017
O_2	0.069	2.7×10^{12}	58	950	0.00016
H_2O	0.208	1.13×10^{13}	47	320	0.00053
CO_2	0.035	1.2×10^{12}	161	1170	0.0014

1 Mb = 10^{-18} cm^2

C. Scattering

It is convenient to express the amount of scattering from an extended source such as the illuminated contamination cloud around a spacecraft in units of brightness of the solar disc $B_\odot$. Given a column density N_c, the B is

$$\frac{B}{B_\odot} = \omega_\odot N_c \left\langle \left(\frac{d\sigma}{d\Omega}\right)_\theta \right\rangle$$

where $\omega_\odot$ is the solid angle subtended by the solar disc which is 6×10^{-5} steradians.

The differential cross section $(d\sigma/d\Omega)_\theta$ is a function of particle size and viewing angle (angle between the line of sight and the sun). The brackets indicate an average over the total size distribution.

For particulates whose radii a are small compared to λ, the scattering cross section is given by Rayleigh theory [7],

$$\left(\frac{d\sigma}{d\Omega}\right)_{\text{Rayleigh}} = 8\pi^4 \frac{a^6}{\lambda^4} \left| \frac{m^2 - 1}{m^2 + 2} \right|^2 (1 + \cos^2 \theta)$$

where m is the index of refraction (m = 1.33) for ice. For molecular scattering, the a^6 times the bracket term is replaced by the square of the polarizability, $(1.76 \times 10^{-24}$ $cm^3)^2$ for most molecules.

For particles with $a >> \lambda$, the scattering cross section may be approximated by diffraction theory for small angles:

$$\left(\frac{d\sigma}{d\Omega}\right)_{\text{dif}} = \frac{\pi^2 a^4}{\lambda^2} \left| \frac{2 J_1(x)}{x} \right|^2$$

where J_1 is a Bessel function and $x = 2\pi a/\lambda \sin\theta$. For θ small, $x << 1$ and

$$J_1(x) \rightarrow \frac{x}{2} - \frac{x^3}{16} + \ldots .$$

The cross section becomes

$$\left(\frac{d\sigma}{d\Omega}\right)_{\text{dif}} = \frac{\pi^2 a^4}{\lambda^2} \left(1 - \frac{x^2}{4} + \ldots\right) .$$

For values of θ such that $x >> 1$, the asymptotic form of the Bessel function is useful. This gives

$$\left(\frac{d\sigma}{d\Omega}\right) = \frac{a\lambda}{2\pi^2 |\sin^3 \theta|} .$$

A useful interpolation formula is

$$\left(\frac{d\sigma}{d\Omega}\right)_{\text{dif}} \approx \frac{3.26\,\pi\, a^4}{\lambda^2} \left[\frac{1}{1 + 4\left(\frac{\pi a \theta}{\lambda}\right)^3} \right] .$$

For large θ and for $a >> \lambda$, the dominant scattering mode will be reflection. For a Lambertian sphere,

$$\left(\frac{d\sigma}{d\Omega}\right)_{ref} = \frac{2\,A\,a^2}{3\,\pi}\,(\sin\theta - \theta\cos\theta) \quad ,$$

where A is the albedo.

For cases where $a \approx \lambda$, the complete Mie theory must be used. This requires extremely tedious computations. Fortunately, the results of these computations are available in tables [9]. However, seldom are parameters such as size, shape, and complex index of refraction well enough known to justify the computational time required for the Mie theory. For most cases, an interpolation formula of the form

$$\left(\frac{d\sigma}{d\Omega}\right)^{-1}_{effective} = \left(\frac{d\sigma}{d\Omega}\right)^{-1}_{Rayleigh} + \left[\left(\frac{d\sigma}{d\Omega}\right)_{diff} + \left(\frac{d\sigma}{d\Omega}\right)_{ref}\right]^{-1}$$

will provide excellent agreement with smoothed Mie theory results. Figure 5 shows such comparisons. It might be noted that the scattering predicted by the above model is greater than predicted by Mie theory for large θ. This is because Mie theory considers a perfectly smooth transparent sphere. For ice crystals released in space, the surface will most likely be diffuse and the Lambertian sphere approximation is applicable.

Scattering estimates at small sun angles for various assumptions of particle size are shown in Table 6.

Energetic particles such as X rays with energies that are large compared to electron binding energies can be treated as scattering from a cloud of free electrons for which the Thompson theory applies:

$$\left(\frac{d\sigma}{d\Omega}\right)_{X\text{-ray}} = Z^2 \left(\frac{e^2}{mc^2}\right)^2 \frac{1}{2}(1 + \cos^2\theta)$$

where $(e^2/mc^2) = 2.82 \times 10^{-13}$ cm for electrons. The Z^2 term indicates that the Z electrons per atom oscillate coherently. This will be the case if the particle is smaller than λ or if θ is small.

The expected scattering for X rays is also indicated in Table 6.

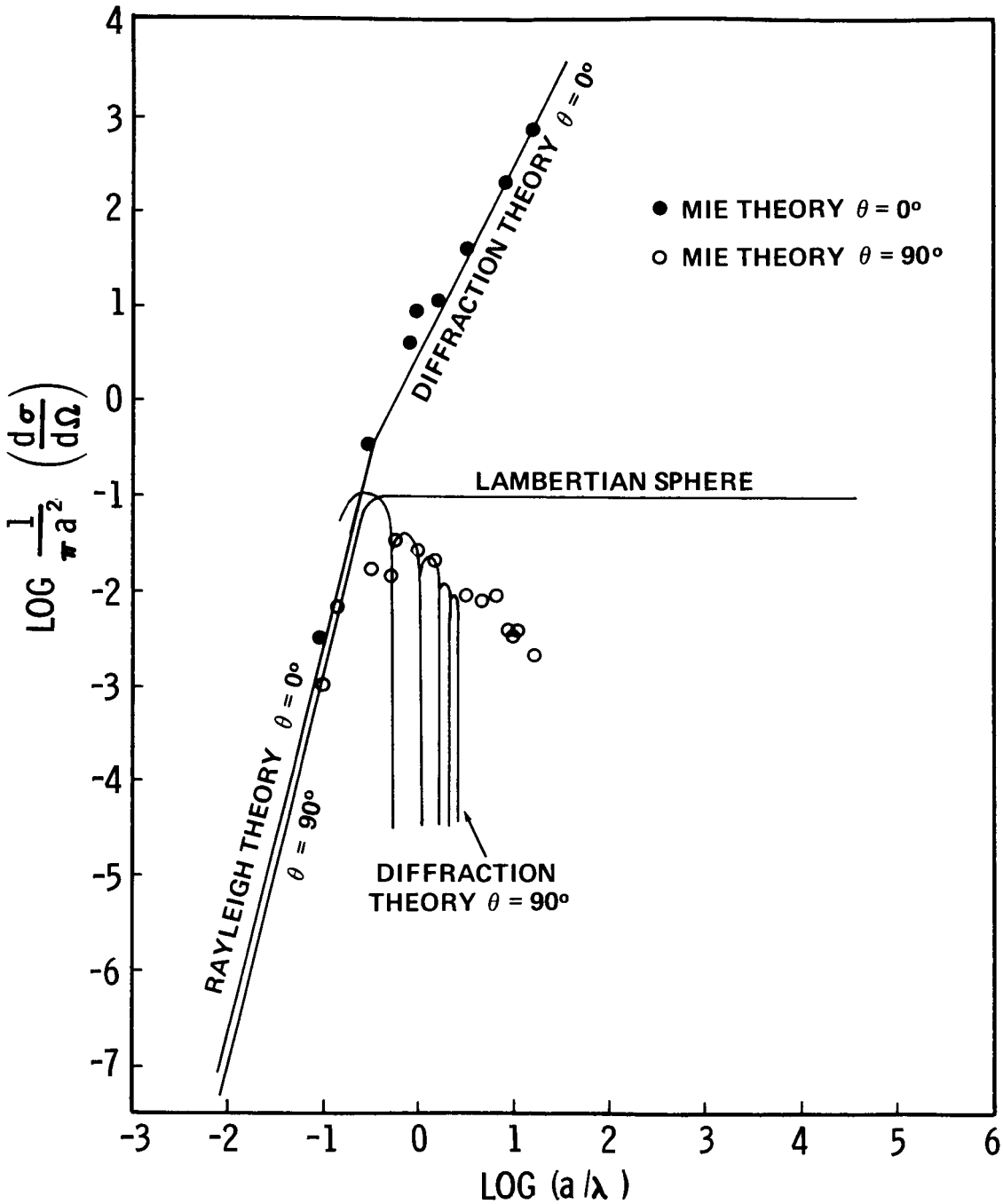

Figure 5. Scattering cross sections for spherical ice particles normalized by the geometrical cross section for scattering angles of 0 deg (forward scattering) and 90 deg. (Except for the region in which $\alpha \approx \lambda$, Rayleigh or diffraction theory gives an excellent approximation to the Mie theory and provides a convenient method for making order of magnitude estimates.)

D. Control Measures

From the preceding discussions, it was shown that molecular scattering from the induced atmosphere around a spacecraft as large and complex as Skylab is inconsequential. The particulate scattering can be a severe problem, particularly when it is necessary to conduct observations near the sun. For such application, no liquid water dumps should be performed.

It was originally thought that water from the Environmental Control System (ECS) condensate could be disposed of by overboard dumps at high velocity to assure rapid clearing. It was later realized that large ice deposits could build up in the vicinity of the nozzle and, instead of a sharp, well defined cutoff, particle production could continue for very long times after the dump. Figure 6 shows an ice cone buildup around the urine dump nozzle on Apollo. Figure 7 shows the actual versus predicted clearing times for an Apollo liquid dump.

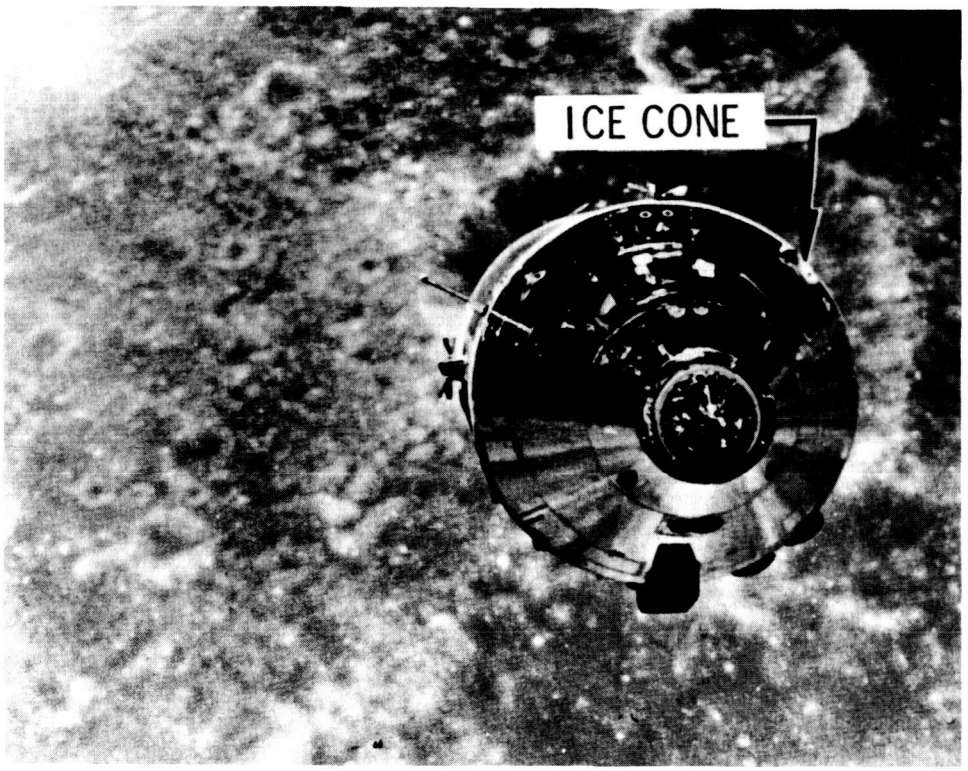

Figure 6. Apollo 10 Command Module showing the ice cone formed around the urine dump nozzle.

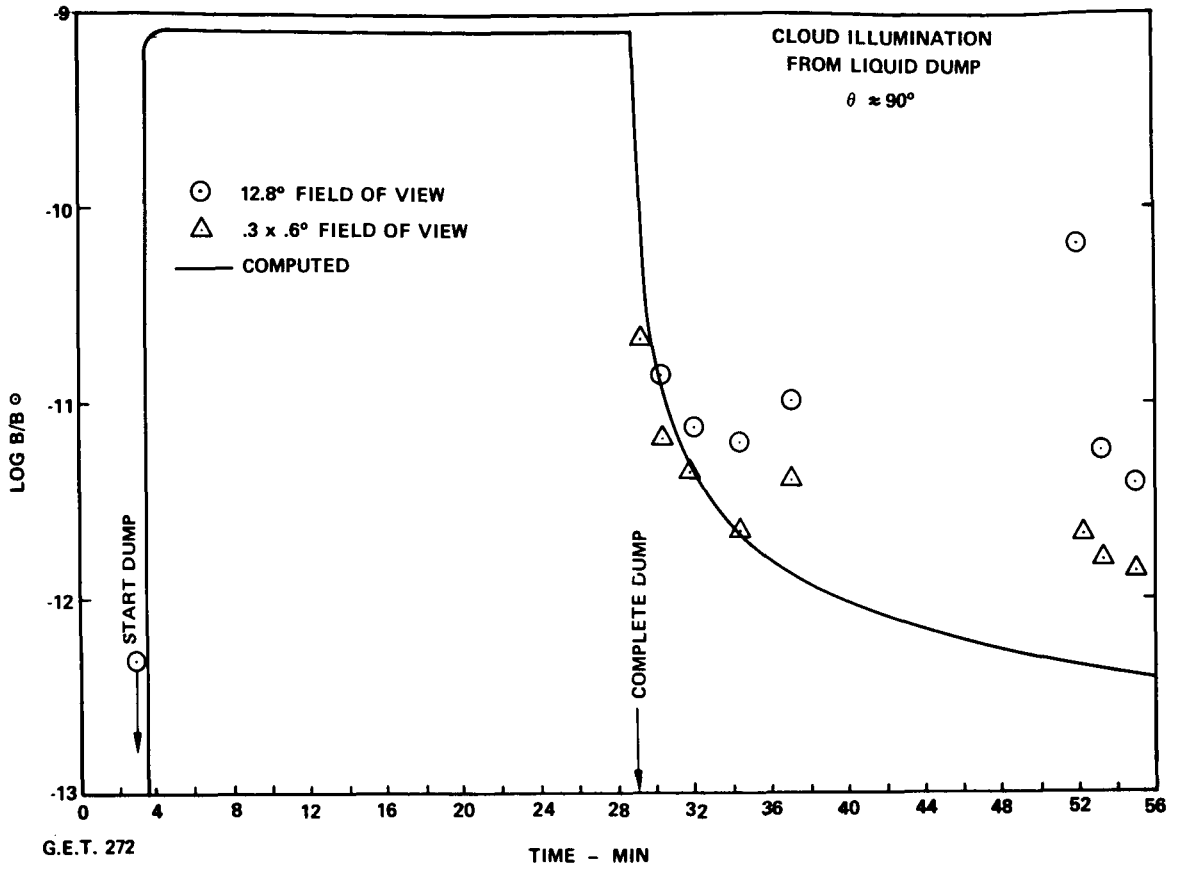

Figure 7. Observed and computed clearing time for approximately 12 kg of liquid dumped throughout a 20-min time interval during the Apollo 15 mission. (The decay at the dump termination is reasonably well predicted by the theory, but the fact that material continues to leave the spacecraft after the dump makes the clearing time much longer than anticipated.)

This could severely interfere with ATM observing time; therefore, it was decided to eliminate the overboard dumps, and all water is now dumped into the OWS storage tank. This presented several problems that required solution. It is necessary to vent the OWS tank to prevent possible buildup of pressure from bacterial action in the waste material that could result in leakage into the crew compartment. To avoid the possibility of dumping liquid water or saturated vapor through the external vents, the flow rate of water into the tank must be controlled to keep the partial pressure below the triple point. Large quantities of ice will be formed when the water is dumped into the tank which must be kept from finding its way through the vents. This is accomplished by separating the region near the dump lines from the main tank volume and the main tank volume from the vent ports by extremely fine mesh screens. A diagram of the tank geometry is shown in Figure 8. Figure 9 shows an electron micrograph of the screen itself. The mesh has nominal size of 2 microns and an absolute size of 9 microns.

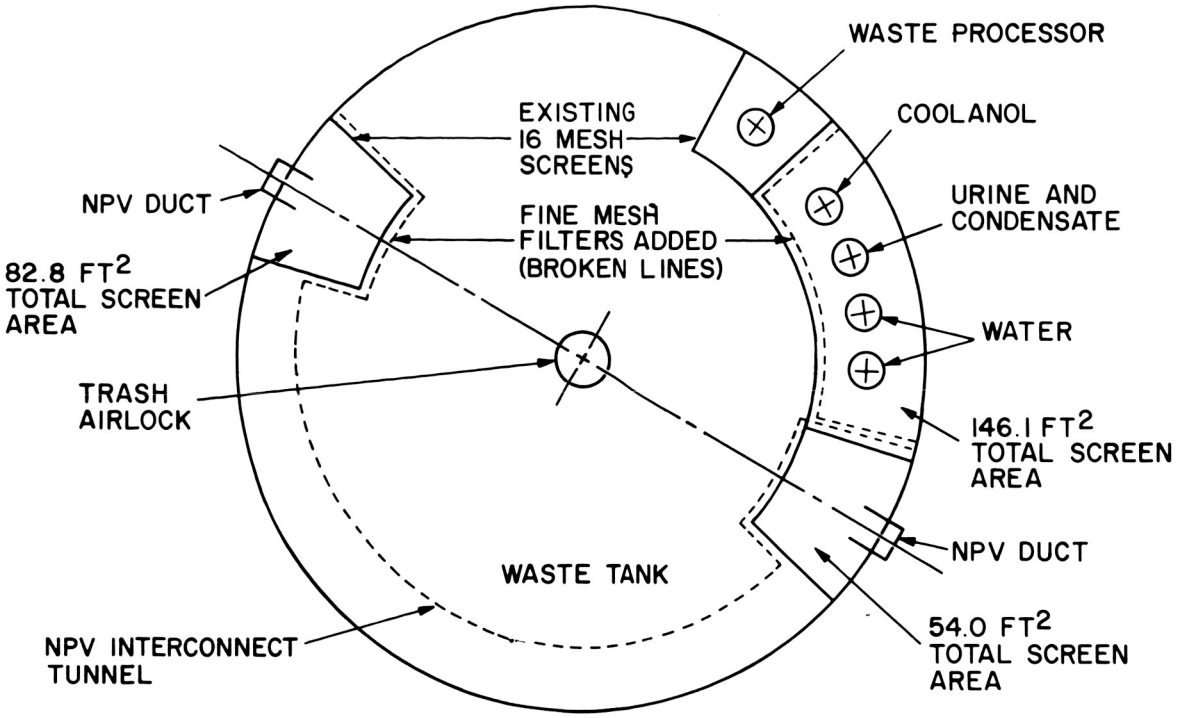

Figure 8. Skylab waste tank configuration showing location of nozzles and filter screens.

Figure 9. Scanning electron micrograph (300X) of the stainless steel "Dutch twill" screens used as filters in the Skylab waste tank. (The small particles trapped in the screen resulted from a urine flow test.)

This concept was successfully demonstrated in the Skylab Contamination Ground Test Program conducted at Martin Marietta Corporation. During normal as well as contingency operation of the Skylab OWS waste tank, the screens were extremely successful in preventing particulate matter from emerging through the vent [10]. The maximum particle production rate was only 40 per sec, with a nominal rate of 20 per sec. Of the particles, 95 percent was between 0.1 and 1.6 microns. This corresponds to a mass flux of 10^{-11} gm/sec. Velocities ranged from 0.5 to 10 m/sec. The estimated scattering shown in Table 6 is completely negligible.

The largest potential source of particulate contamination remaining on Skylab is dust particles that settle on surfaces during assembly, storage, and launch operations. Despite the cleanliness precautions, it must be remembered that clean rooms are not all that clean. A 10K room has 3.53×10^5 particles/m^3 larger than 0.5 micron and 2295 particles/m^3 larger than 5 microns. A very large number of particles still can be deposited, particularly on a dielectric surface that is located where moving air is circulated over it. Despite the elaborate cleanliness precautions taken in a clean room, a worker still emits 500 000 to 1 000 000 particles larger than 0.3 micron per minute [11]. In a conventional clean room, the presence of this man will raise the local particle count by as much as 3.15×10^5 to 6.3×10^5 particles/m^3. How many such particles will actually deposit on spacecraft surfaces and how they will behave when subjected to the space environment is difficult to estimate.

Federal Standard 209 specified that a class 10K clean room must have fewer than 10^4 particles/ft^3 larger than 0.5 micron in diameter and fewer than 65 particles/ft^3 larger than 5 microns in diameter. Assuming a power law distribution function, the cumulative distribution is given by

$$N > d = 0.0776 d^{-2.187}$$

where $N > d$ is the number of particles per cubic centimeter larger than d, and d is the diameter in microns. For class 100K and class 100, the coefficient may be multiplied or divided by 10 or 100, respectively. Assuming spherical particles of 1 gm/cm^3 density, the dust in a 100K clean environment corresponds to a pollution index of 3.7 $\mu g/m^3$, which is more than 10 times smaller than ambient.

The dust fall on a surface is the product of the number density and the velocity. For still air, the fall velocity is given by Stokes' formula,

$$v_{fall} = \frac{\rho d^2 g}{18\mu} .$$

Using $\mu = 1.813 \times 10^{-4}$ poise for air at 20°C, and $\rho = 1$ gm/cm^3

$$v_{fall} = 0.003\ d^2 \text{ (cm/sec)}$$

with d expressed in microns.

Integrating the product of the velocity and the number density distribution over the size spectrum yields

$$\Phi_{>d} = 235\ d^{-0.187} \ ;\ 0.5\ \mu \leqslant d \leqslant 5\ \mu$$

where $\Phi_{>d}$ is the number of particles per square centimeter day with diameters greater than d microns falling on a horizontal surface. The expected number for various size intervals is shown in Table 8 for class 100K and 10K clean rooms.

In one-year exposure to a 100K environment, a surface will collect 3.41×10^5 particles/cm^2 ranging from 0.5 micron to 5 microns in diameter. This represents 2.75 μg/cm^2, or 1.26 percent coverage. Representing a spacecraft by a 20-m diameter sphere and assuming the particles come off uniformly for 7 days after orbital insertion with a relative velocity of 0.1 m/sec, the resulting $B/B_\odot$ is 4.7×10^{-9} at $\theta = 0$ deg.

TABLE 8. DUST-ACCUMULATION (particles/cm^2/day)

Size Interval	100K	10K
0.5 to 10	325	32.5
1.0 to 2.0	285	28.5
2.0 to 3.0	151	15.1
3.0 to 4.0	100	10.0
4.0 to 5.0	74	7.4

IV. SUMMARY

Details of the mechanisms by which scientific experiments can become contaminated have been developed. Deposition of contamination film on optics can be controlled by: (1) isolating critical optical surfaces from the rest of the spacecraft; (2) using as little nonmetallic material as possible, particularly near or in line of sight of optical surfaces; (3) choosing nonmetallics carefully to avoid materials with high vapor pressures; (4) vacuum baking materials before use to drive off the more volatile outgassing products; (5) keeping critical surfaces warmer than surroundings; (6) avoiding having nonmetallic material run at elevated temperatures; (7) paying special attention to optics exposed to intense ultraviolet, X-ray, or particulate radiation; (8) not permitting any source of water vapor such as multilayer insulation to vent near cooled detectors; and (9) directing RCS plumes away from critical surfaces and providing suitable covers that can be closed during RCS maneuvering.

For control of particulate contaminants: (1) maintain stringent cleanliness requirements on all spacecraft surfaces; (2) provide protection such as dust covers for critical surfaces during launch; (3) protect critical surfaces during storage in clean rooms; (4) design critical surfaces for easy access so that final inspection and cleaning may be made just prior to flight; (5) avoid dumping liquid waste overboard – covert it to vapor phase first; and (6) make sure there are no loose edges of multilayer insulation or fabric material that may create particles by abrading.

The most important thing is to develop an awareness of contamination problems and always be alert to uncover unsuspected sources and effects.

George C. Marshall Space Flight Center
National Aeronautics and Space Administration
Marshall Space Flight Center, Alabama 35812, June 1973
502-21-28-0000

APPENDIX A. CONDITIONS FOR BUILDUP OF DEPOSITION

For a contamination film to continue to grow, it is necessary for molecules to arrive faster than they leave, which requires the partial pressure of the contaminating species to be above its vapor pressure P_V at the temperature of the surface in question. If the pressure is lower than P_V, the number on the surface will reach an equilibrium value given by the Brunauer, Emmett, and Teller (BET) equation [12]; i.e.,

$$\frac{\sigma}{\sigma_S} = \frac{C\, P/P_V}{(1 - P/P_V)\,[1 + (C - 1)\, P/P_V]} \tag{A-1}$$

where σ/σ_S is the number of monolayers and C is given approximately by $\exp[(H_1 - H_V)/RT]$. H_V is the heat of vaporization of the contaminant, and H_1 is the binding energy of the contaminant on the substrate. For some materials, $H_1 > H_V$ because of chemisorption on the surface. But, even if C is very large, the BET equation becomes

$$\frac{\sigma}{\sigma_S} \quad C \Rightarrow \infty \quad \frac{1}{1 - P/P_V} = -\frac{t_1}{\tau_1} \quad . \tag{A-2}$$

Therefore, unless P is very nearly equal to or greater than P_V, only a few monolayers will deposit.

There is one possibility of producing contamination buildup at pressures below the vapor pressure: the contaminant could cross-link or polymerize, forming a new material that is much more stable than the original species. Solar ultraviolet or particle radiation could provide the energy required for this polymerization. If this happens, the buildup is given by equation (1), with the stay time τ corresponding to the polymerized material.

APPENDIX B. RETURN FLUX FROM ATMOSPHERIC SCATTER

The following procedure is used to compute the number of molecules back-scattered from a spacecraft by atmospheric collisions.

Assume that molecules leave the spacecraft isotropically with average radial velocity v_r. Let the spacecraft be represented by a sphere with radius R. The number density as a function of radial distance r is found from equation (19):

$$N(r) = \frac{n_{evap} R^2}{v_r r^2} \quad . \tag{B-1}$$

Consider the atmosphere relative to the spacecraft a monoenergetic molecular beam with flux $n = N_a v_a$ where N_a is the number density and v_a is the orbital velocity. The probability per unit time for an outgoing molecule to be scattered into solid angle $d\Omega$ in the direction θ

$$d\dot{Q} = n\left(\frac{d\sigma}{d\Omega}\right)_\theta d\Omega \tag{B-2}$$

where $(d\sigma/d\Omega)_\theta$ is the differential cross section.

The element of solid angle subtends:

$$d\Omega = \frac{\cos\phi \, dA}{r'^2} \tag{B-3}$$

where ϕ is the angle between $\vec{r}'$ and the normal to the surface in question.

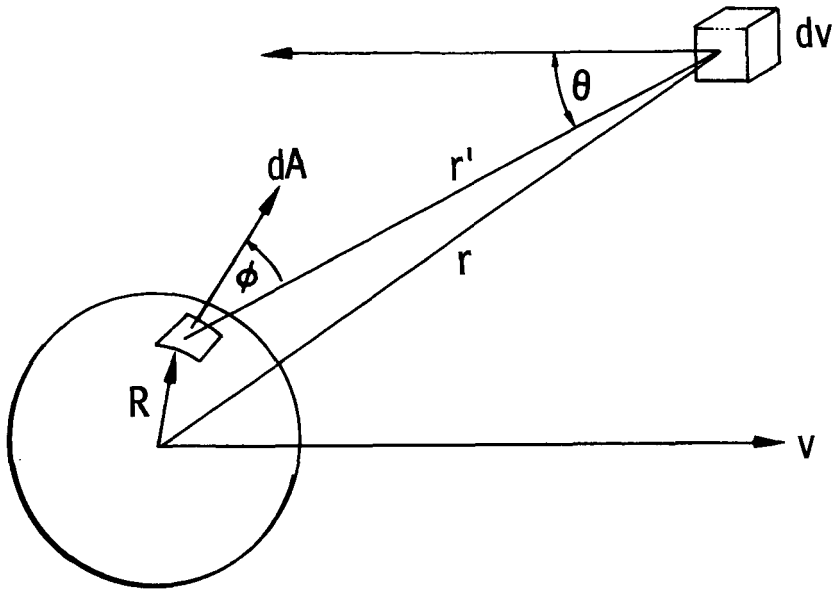

Therefore, the return flux from an element of volume is given by the number of outgoing molecules in the element of volume times the probability per unit time of their being scattered into the area element dA , or

$$dn_{ret} = N(r)\, dV\, \frac{d\dot{Q}}{dA} \tag{B-4}$$

which using equations (B-1), B-2), and B-3) becomes

$$dn_{ret} = \frac{n_{evap}\, R^2}{v_r\, r^2}\, \frac{N_a\, v_a}{r'^2}\, \cos\phi\, \left(\frac{d\sigma}{d\Omega}\right)_\theta\, dV \quad . \tag{B-5}$$

The analysis is greatly simplified by choosing the area in question at the stagnation point, resulting in $\phi = \theta$. Now the integration over all volume is performed by integrating over r' and θ .

$$\frac{n_{ret}}{n_o} = \frac{2\pi\, R^2\, N_a\, v_a}{v_r} \int_0^{\pi/2} d\theta \int_0^{\infty} \frac{dr' \sin\theta\, \cos\theta}{(R^2 + r'^2 + 2\, R\, r' \cos\theta)} \left(\frac{d\sigma}{d\Omega}\right)_\theta \quad . \tag{B-6}$$

In the center of mass system, the collision can be considered isotropic. Therefore,

$$\left(\frac{d\sigma}{d\Omega}\right)_{c/m} = \frac{\sigma_a}{4\pi} \tag{B-7}$$

where σ_a is the collision cross section $\pi/4\,(d_1 + d_2)^2$ where d_1 and d_2 are the diameters of the colliding and collided molecules.

To a very good approximation, the velocity of the molecules leaving the spacecraft may be ignored in regard to the speed of the atmospheric molecules. Therefore, the transformation from the center of mass system to the lab system may be used.

The cross section transforms according to

$$\left(\frac{d\sigma}{d\Omega}\right)_{lab} 2\pi \sin\theta \, d\theta = \left(\frac{d\sigma}{d\Omega}\right)_{c/m} 2\pi \sin\theta^* \, d\theta^* \qquad \text{(B-8)}$$

and the scattering angle transforms according to

$$\theta^* = \pi - 2\theta \qquad \text{(B-9)}$$

where θ is the angle the stationary particle (in this case, the outgassing molecule) is scattered relative to the colliding molecule.

From this, the transformation becomes

$$\left(\frac{d\sigma}{d\Omega}\right)_{lab} = 4\cos\theta \left(\frac{d\sigma}{d\Omega}\right)_{c/m} = \frac{4\cos\theta\ \sigma_a}{4\pi} \qquad \text{(B-10)}$$

Putting this in equation (B-6) gives

$$\frac{n_{ret}}{n_{out}} = \frac{2R^2 N_a v_a \sigma_a}{v_r} \int_0^{\pi/2} d\theta \int_0^{\infty} dr' \frac{\sin\theta \cos^2\theta}{R^2 + r'^2 + 2Rr'\cos\theta}$$

$$= \frac{2R^2 N_a v_a \sigma_a}{v_r} \int_0^{\pi/2} \frac{\theta \cos^2\theta \, d\theta}{R}$$

$$\frac{n_{ret}}{n_{out}} = \left(\frac{\pi^2 - 4}{8}\right) \frac{R N_a v_a \sigma_a}{v_r} \qquad \text{(QED)} \qquad \text{(B-11)}$$

REFERENCES

1. Reynolds, J.M.; Fields, S.A.; and Wilson, R.M.: X-Ray Reflection Efficiency of Ni-Coated Quartz Flats. NASA TM X-64747, May 10, 1973.

2. McKeown, D. and Corbin, W.E., Jr.: Space Measurements of the Contamination of Surfaces by OGO-6. Paper presented to the Space Simulation Conference, National Bureau of Standards, Gaithersburg, Md., September 1970.

3. Robertson, S.J.: Backflow of Outgas Contamination onto Orbiting Spacecraft as a Result of Intermolecular Collisions. LSMC-HREC D 306000, Lockheed Missiles and Space Co., Contract NAS8-26554, June 1972.

4. McKeown, D. and Corbin, W.E., Jr.: Removal of Surface Contamination by Plasma Sputtering. Proceedings of AIAA 6th Thermophysics Conference, U. of Tenn. Space Institute, Tullahoma, Tenn., April 1971.

5. Hoffman, J.H.; Hodges, R.R.; and Evans, D.E.: Lunar Orbital Mass Spectrometer Experiment. Apollo 15 Preliminary Science Report, NASA SP-289, 1972.

6. West, W.S.; Gore, J.V.; Kasha, M.A.; and Bilsky, H.W.: Spacecraft Charge Buildup Analysis. NASA SP-276, 1971.

7. Buffalano, A.C.; Kratage, M.L.; and Sharma, R.D.: Interpretation of Visual Observations of Apollo Water Dumps – Case 340. Bellcomm Memorandum B7107014, July 1971.

8. McPherson, D.G.: Apollo Telescope Mount Extended Applications Study. NASA CR-61173, May 1967.

9. Bicket, N.A. and Gary, G.A.: Mie Scattering: A Computer Program and an Atlas. NASA TM X-53951, September 1969.

10. Skylab Orbital Assembly Systems, Design Certification Review Report, Contamination. Published by Martin Marietta Corp., August 1972.

11. Austin, P.R.: Personnel and Their Contribution to Product Contamination. Contamination Control, October 1965, p. 45.

12. Brunauer, S.: The Absorption of Gases and Vapors. Oxford University Press, London, 1943.